SIMULTANEOUS INVERSE ESTIMATION OF SOIL HYDRAULIC AND SOLUTE TRANSPORT PARAMETERS FROM TRANSIENT FIELD EXPERIMENTS: HOMOGENEOUS SOIL

F. Abbasi, J. Simunek, J. Feyen, M. Th. van Genuchten, P. J. Shouse

ABSTRACT. *Inverse estimation of unsaturated soil hydraulic and solute transport properties has thus far been limited mostly to analyses of one–dimensional experiments in the laboratory, often assuming steady–state conditions. This is partly because of the high cost and difficulties in accurately measuring and collecting adequate field–scale data sets, and partly because of difficulties in describing spatial and temporal variabilities in the soil hydraulic properties. In this study, we estimated soil hydraulic and solute transport parameters from several two–dimensional furrow irrigation experiments under transient conditions. Three blocked–end furrow irrigation experiments were carried out, each of the same duration but with different amounts of infiltrating water and solutes resulting from water depths of 6, 10, and 14 cm in the furrows. Two more experiments were carried out with the same amounts of applied water and solute, and hence for different durations, on furrows with water depths of 6 and 10 cm. The saturated hydraulic conductivity (K_s) and solute transport parameters in the physical equilibrium convection–dispersion (CDE) and physical nonequilibrium mobile immobile (MIM) transport models were inversely estimated using the Levenberg–Marquardt optimization algorithm in combination with the HYDRUS–2D numerical code. Soil water content readings, cumulative infiltration data, and solute concentrations were used in the objective function during the optimization process. Estimated K_s values ranged from 0.0389 to 0.0996 cm min^{-1}, with a coefficient of variation of 48%. Estimated immobile water contents (θ_{im}) were more or less constant at a relatively low average value of 0.025 cm^3 cm^{-3}, whereas the first–order exchange coefficient (ω) varied between 0.10 and 19.52 min^{-1}. The longitudinal dispersivity (D_L) ranged from 2.6 to 32.8 cm, and the transverse dispersivity (D_T) ranged from 0.03 to 2.20 cm. D_L showed some dependency on water level and irrigation/solute application time in the furrows, but no obvious effect was found on K_s and other transport parameters, most likely because of spatial variability in the soil hydraulic properties. Agreement between measured and predicted infiltration rates was satisfactory, whereas soil water contents were somewhat overestimated, and solute concentrations were underestimated. Differences between predicted solute distributions obtained with the CDE and MIM transport models were relatively small. This and the value of optimized parameters indicate that observed data were sufficiently well described using the simpler CDE model, and that immobile water did not play a major role in the transport process.*

Keywords. *Furrow irrigation, Homogeneous soil, Inverse solution, Solute transport, Water flow.*

While considerable progress has been made during the past several decades in describing and modeling water flow and solute transport processes under controlled, often steady–state, conditions at the laboratory scale, detailed analyses of field–scale experiments remain limited, mostly because of labor and cost requirements, but also because of inherent complications posed by field–scale heterogeneity. For example, the unsaturated soil hydraulic properties can change by several orders of magnitude, even over relatively short distances (Biggar and Nielsen, 1976; Bresler et al., 1984), thus making it difficult to assign values that are applicable at the field scale.

A wide range of models exists for simulating water flow and solute transport in the vadose zone. Addiscott and Wagenet (1985) gave a review of one–dimensional (1–D) transport models. They compared and classified the models as being deterministic or stochastic, mechanistic or functional, numerical or analytical, and research or management oriented. They also discussed the degree of complexity, flexibility, transferability, and usefulness of these models for field conditions. One–dimensional water flow and solute transport models (such as those developed by Jarvis et al., 1991; Sulekha and Duijnisveld, 1998; Shao et al., 1998; Simunek et al., 1998; among others) are useful for many applications. While requiring less expertise in programming, fewer input data, and less computer time and memory than two–dimensional (2–D) models, 1–D approaches generally do not accurately describe geometry and thus the dynamics of water and solutes during irrigation using furrows, drippers, perforated tubes, and porous lines, or some other method. In such cases, flow and transport are two– or even three–dimen-

Article was submitted for review in July 2002; approved for publication by the Soil & Water of ASAE in May 2003.

The authors are **Fariborz Abbasi,** Soil Physicist, and **Jan Feyen,** Professor, Institute for Land and Water Management, Katholieke Universiteit Leuven, Belgium; and **Jirka Simunek,** Soil Physicist, **Martinus Th. van Genuchten,** Research Leader, and **Peter J. Shouse,** Soil Physicist, USDA–ARS, George E. Brown Jr. Salinity Laboratory, Riverside, California. **Corresponding author:** Jan Feyen, Institute for Land and Water Management, Vital Decosterstraat 102, 3000–Leuven, Belgium; phone: +32–16–329756; fax: +32–16–329760; e–mail: jan.feyen@agr.kuleuven.ac.be.

sional (3–D), thus requiring a multi–dimensional simulation model.

A number of 2–D (e.g., Neuman et al., 1975; Simunek et al., 1999a) and 3–D (Wu and Chieng, 1995a, 1995b; Russo et al., 1998) models currently exist, with the governing equations generally being solved using a variety of finite difference, finite element, or other numerical methods (e.g., Segol, 1994; Forsyth et al., 1995; van Genuchten and Sudicky, 1999, Kees and Miller, 2001). Multi–dimensional models are more suitable for studying the effects of soil spatial variability on water flow and solute transport at the field scale. Unfortunately, field applications of such models remain limited since they generally require large amounts of input data and field measurements, and consequently can become quite costly to implement. For example, Wu and Chieng (1995a, 1995b) developed a three–dimensional multi–component solute transport model. The finite element model was used successfully to simulate chemical reactions such as acid–base reaction, complexation, ion exchange, precipitation and dissolution, as well as heat transfer and vapor movement. Loretta and Wu (1999) later used this model to study the transport of four heavy metals through a clay barrier. Russo et al. (1998) similarly presented a 3–D model for simulating water flow and solute transport within the unsaturated zone. They used a fully implicit Euler scheme to solve the water flow equation, while solute transport was approximated by an operator–splitting approach. Application to bromacil transport showed that the patterns of moisture contents, pressure heads, pressure gradients, hydraulic conductivities, and root–water uptake were considerably affected by spatial heterogeneity in the soil hydraulic properties.

Of special interest to this study is the HYDRUS–2D code developed by Simunek et al. (1999a). HYDRUS–2D is a Microsoft Windows–based modeling environment for analyzing water flow and solute transport in 2–D variably saturated porous media, as well as for inverse estimation of soil hydraulic and/or solute transport properties. The governing equations are numerically solved using Galerkin–type linear finite elements, while the Levenberg–Marquardt algorithm (Marquardt, 1963) is used for parameter optimization. The model has been successfully used in many laboratory and field studies (e.g., Gribb, 1996; Simunek and van Genuchten, 1996, 1997; Kodesova et al., 1998, 1999) to optimize soil hydraulic properties. For example, Simunek and van Genuchten (1996) showed that measured infiltration data using a tension disc infiltrometer at constant tension did not provide enough information to inversely estimate soil hydraulic properties, whereas using infiltration data at multiple tensions yielded good estimates of the soil hydraulic properties (Simunek and van Genuchten, 1997). The model was also successfully used to inversely estimate soil hydraulic properties from cone permeameter experiments (Gribb, 1996; Kodesova et al., 1998, 1999; Simunek et al., 1999b). In other studies, Wang et al. (1997) used the CHAIN–2D model (Simunek and van Genuchten, 1994), an early version of the HYDRUS–2D, to investigate the effects of different irrigation methods and spatial variability in the saturated hydraulic conductivity on subsurface solute transport. Mohanty et al. (1997, 1998) similarly used CHAIN–2D to study water flow and nitrate transport in a soil profile with subsurface tile drains. The model predicted nitrate concentrations in the soil profile reasonably well, but underestimated nitrate flux concentrations in the subsurface tile drain, and overestimated those in piezometers.

Despite considerable efforts in studying solute transport at the field scale during transient flow, particularly during the past 20 years, the implications of using different irrigation methods on subsurface solute transport have received relatively little attention. The limited studies available in the literature suggest that transport processes can be significantly affected by irrigation regime and application method (Bowman and Rice, 1986; Jaynes et al., 1988; Wang et al., 1997). In an extensive furrow irrigation study, Abbasi et al. (2003) recently showed that water flow depth and irrigation/solute application time both play a major role in transporting and distributing water and solutes below the furrows. The main purpose of this study was to quantify soil hydraulic and solute transport properties from various 2–D field experiments on blocked–end furrows under transient conditions. The parameter optimization features of HYDRUS–2D were used to inversely estimate K_s and the transport parameters in the classical convection–dispersion (CDE) and physical nonequilibrium mobile–immobile (MIM) solute transport models assuming the presence of a homogeneous soil profile. While the CDE model holds for relatively uniform flow conditions, the MIM model also considers nonequilibrium and/or preferential flow associated with the presence of relatively immobile liquid regions in the soil. The MIM model reduces to the CDE model when nonequilibrium is not present.

Materials and Methods

Field Experiments

Five field experiments on short blocked–end furrows were conducted at the Maricopa Agricultural Center (MAC) in Phoenix, Arizona, on a non–vegetative Casa Grande sandy loam soil (fine–loamy, mixed, hyperthermic Typic Natrargids). Experiments were carried out in plots made up of three furrows approximately 20 cm deep and spaced 1.0 m apart. The monitored center furrow of each plot was a non–wheel furrow, with a wheel track furrow on each side of the monitored furrow. The blocked portion of the furrows was 3 m in length. Details about the experiments can be found in Abbasi et al. (2003). Below we briefly discuss only those parts of the experiments that are directly related to this study.

Two series of experiments were carried out. We first performed same–duration (SD) experiments involving three flow depths (6, 10, and 14 cm) used in two successive irrigations, 10 days apart. The first irrigation took place in two phases. During the first phase, water was applied for 60 min (the same for all three experiments) to wet the soil profile. Water was then removed from the furrows and measured using an electric scale. During the second phase, water amended with $CaBr_2$ was applied for 30 min again the same for the three indicated plots. Water in the furrow was again removed and the amount determined. The second irrigation utilized the same depths of unamended water as employed during the first irrigation, and lasted 90 min. As for the first irrigation, water stored in the furrow was pumped out and measured at the end of the experiment.

The second series of experiments involved similar amounts of applied water and solutes (SWS). The amount of water applied was the same as that infiltrated for the 14 cm depth treatment of the SD experiments. Water levels of 6 and 10 cm were used in this case. The first irrigation was carried out in two steps, similarly to the SD scenarios, with unamended water being applied first followed by bromide–amended water, except that the irrigation times were adjusted for each of the water levels such that predefined amounts of water, obtained from the previous experiment with 14 cm flow depth, infiltrated. The second irrigation used unamended water applied with the same water levels as for the first irrigation, but with times adjusted so that again the same amount of water infiltrated during the second irrigation as for the 14 cm depth treatment in the first set of experiments. As stated above, the 14 cm flow depth experiment plays as a transient experiment between the SD and SWS scenarios.

A set of five neutron probe access tubes (each 3.3 m in depth) was installed to measure soil water contents at different locations perpendicular to the axis of the monitored furrows. The neutron tubes were installed in two rows 50 cm apart in order to avoid mutual effects on the readings (see Abbasi et al., 2003, for details). A site–calibrated neutron probe was used to measure soil water contents. The readings were taken at depths of 20, 40, 60, 80, 100, 140, 180, 220, and 260 cm before each irrigation to provide initial conditions, immediately after each irrigation, then hourly up to 6 hours after each irrigation, and subsequently each 3 hours up to 24 hours. Measurements were later taken 3 to 4 times per day up to 3 days after irrigation, and then 1 to 2 times per day up to the next irrigation. Since neutron probe readings are generally imprecise near the soil surface, water contents of the surface layer (0 to 30 cm) were measured using a site–calibrated time domain reflectometry (TDR) probe. The TDR and neutron probe readings were taken at the same times as indicated above.

Soil samples for analyzing bromide concentrations were taken manually, at depths and locations corresponding to the neutron probe access tube measurements, four times during the experiments, i.e., prior to the experiments as initial values, 5 days after the first irrigation, and 6 and 20 days after the second irrigation. The samples were air dried and crushed to pass a 2 mm sieve. Soil extractions (1:1 weight:volume) were made and analyzed for bromide with a Lachat QuikChem flow injection analyzer using standard colorimetric procedures. In addition, 38 undisturbed soil samples (6 cm long, 5.4 cm diameter soil cores) were collected randomly at different locations and depths (up to 100 cm) for laboratory analyses of the soil water retention curve and the saturated hydraulic conductivity.

The same bromide concentration (10 g L^{-1}) was used in all experiments. Flow depths were kept constant during the irrigation by adjusting the water levels to the desired heights as determined from staff gauges placed at the bottom of the furrows. Geometries of the experimental furrows were determined before each irrigation at two locations along the furrows in order to calculate the volume of water needed to fill the furrow section and to infer geometry parameters required for numerical calculations using HYDRUS–2D. Measured and fitted geometries of the furrows before each irrigation are shown in figure 1.

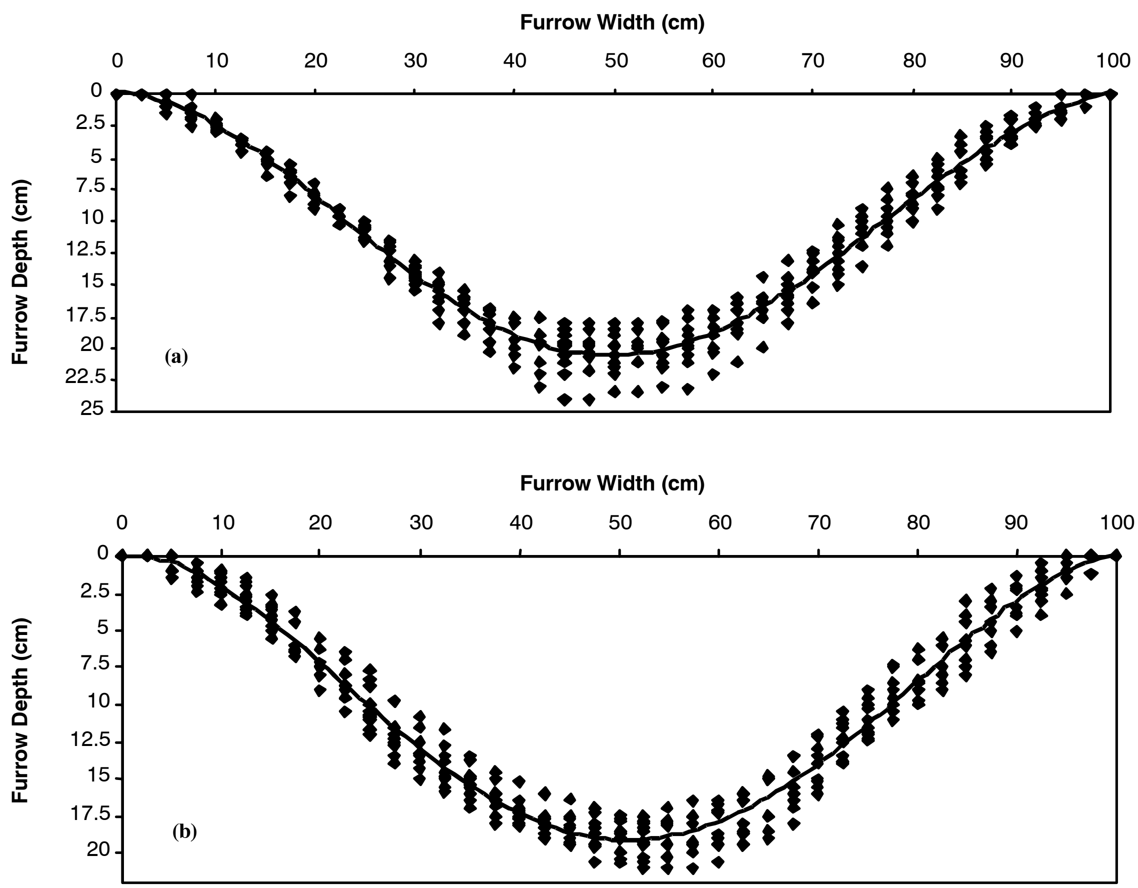

Figure 1. Geometries of the experimental furrows and the fitted profiles. Symbols are the measured data and solid lines are the best fits: (a) before the first irrigation, and (b) before the second irrigation.

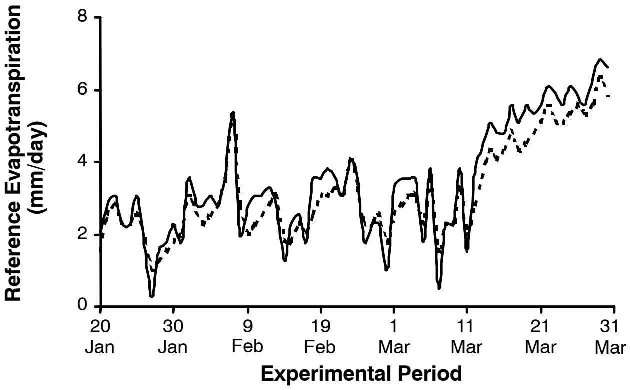

Figure 2. Reference pan evapotranspiration rates and rates estimated using the Penman–Monteith method (dashed line = Penman–Monteith, and continuous line = pan).

All plots were covered with plastic sheets during possible rainfall events to make sure that irrigation was the only source of water during the experiments. Reference evapotranspiration rates from the nearest weather station (approximately 150 m from the experimental field) and estimated evapotranspiration rates using the Penman–Monteith method (Allen et al., 1994) are given in figure 2. The SD and SWS experiments started on 30 January and 26 February 2001, respectively, and each lasted 30 days.

Model Description

Water Flow

Two–dimensional isothermal Darcian flow of water in a variably saturated rigid porous medium is given by the following form of the Richards equation (Richards, 1931):

$$\frac{\partial\theta}{\partial t}=\frac{\partial}{\partial x_i}[K(K_{ij}^{A}\frac{\partial h}{\partial x_i}+K_{iz}^{A})]-\Gamma \quad (1)$$

where

θ = volumetric soil water content ($L^3\ L^{-3}$)
h = pressure head (L)
Γ = sink term (e.g., root water uptake; T^{-1})
x_i = spatial coordinates (L; i = 1, 2)
t = time (T)
$K_{ij}{}^{A}$ and $K_{iz}{}^{A}$ = components of the dimensionless anisotropy tensor K^A
K = unsaturated hydraulic conductivity function ($L\ T^{-1}$) given by:

$$K(h) = K_s K_r(h) \quad (2)$$

where

K_s = saturated hydraulic conductivity ($L\ T^{-1}$)
K_r = relative hydraulic conductivity.

In this study, K^A was assumed to be isotropic. The sink term (Γ) in equation 1 was set to zero since the soil in this study was left bare (no root water uptake).

Soil Hydraulic Properties

The soil water retention curve, $\theta(h)$, was described using the closed–form equation of van Genuchten (1980), and the unsaturated soil hydraulic conductivity function, $K(h)$, was described using the capillary model of Mualem (1976) as follows:

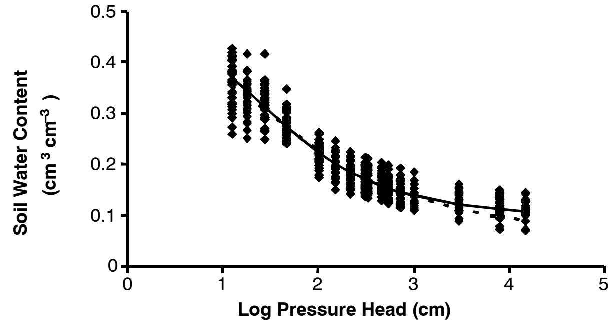

Figure 3. Measured and fitted soil water retention curves (symbols = measured, dashed line = RETC and Rosetta optimization, and continuous line = RETC optimization).

$$\theta(h)=\theta_r+\frac{\theta_s-\theta_r}{(1+|\alpha h|^n)^m} \quad (3)$$

$$K(h) = K_s S_e{}^{l}[1-(1-S_e{}^{1/m})^m]^2 \quad (4)$$

where

$$S_e=\frac{\theta-\theta_r}{\theta_s-\theta_r},\quad m=1-\frac{1}{n},\quad n>1 \quad (5)$$

and

θ_r = residual soil water contents ($L^3\ L^{-3}$)
θ_s = saturated soil water contents ($L^3\ L^{-3}$)
S_e = relative saturation (dimensionless)
m, n, l, α = empirical parameters (m, n, and l dimension–less; α in L^{-1}).

Soil water retention data (fig. 3) were determined on small undisturbed soil samples in the laboratory using Tempe cells (for pressures below 1 bar) and pressure plates (for pressures over 1 bar). The van Genuchten (VG) retention parameters θ_r, θ_s, α, and n were estimated from the measured $\theta(h)$ data using the RETC non–linear optimization program of van Genuchten et al. (1991). The optimized parameters, sum of squared residuals (SSQ), and regression between the observed and estimated values (R^2) are listed in table 1. The optimized value for θ_r (0.10 $cm^3\ cm^{-3}$) was found to be slightly higher than the water contents (approximately 0.090 $cm^3\ cm^{-3}$) of the soil surface layers (0 to 0.20 m) measured at the end of the experiments. For this reason, we also estimated the θ_r using neural network–based pedotransfer functions derived by Schaap et al. (2001) and incorporated into their Rosetta code. Rosetta predicts VG retention parameters and K_s in a hierarchical manner from soil textural class information, soil textural fractions, the bulk density, and one or two water retention points as input (Schaap et al., 2001).

Table 1. van Genuchten soil hydraulic properties obtained with the RETC and Rosetta optimization codes.

Method	θ_r ($cm^3\ cm^{-3}$)	θ_s ($cm^3\ cm^{-3}$)	α (cm^{-1})	n (–)	SSQ[a] (–)	R^2 (–)
RETC	0.10	0.433	0.0758	1.478	0.273	0.92
Rosetta	0.065	0.407	0.0545	1.503	—	—
Rosetta+RETC	0.065[b]	0.407[b]	0.0689	1.37	0.3	0.91

[a] SSQ = sum of squared residuals.
[b] Estimated with Rosetta and used as fixed value for the RETC optimization.

VG parameters estimated with Rosetta (assuming $l = 0.5$ in eq. 4) are given in table 1. Rosetta predicted θ_r, θ_s, and α values that were somewhat lower than those obtained with RETC, while both approaches produced almost the same values for n. The Rosetta values for both θ_r and θ_s agreed well with those reported by Carsel and Parrish (1988). As a result, we used a combination of Rosetta and RETC to finalize the soil hydraulic parameters: θ_r and θ_s were chosen from Rosetta and used as fixed values in RETC to estimate α and n from the measured retention data (the third option in table 1 and fig. 3).

The saturated conductivity (K_s) was measured on undisturbed soil samples (6 cm long and 5.4 cm diameter) using the constant head method. The average K_s from 38 samples was 725 cm day^{-1}, with a coefficient of variation of 73%. The average K_s was much larger than those of most agricultural soils, even coarse–textured soils (e.g., Carsel and Parrish, 1988; Schaap et al., 1998). The large K_s values could have been caused by possible disturbance of the samples during collection and transportation (from the field site in Arizona to the Salinity Laboratory in Riverside, California), measurement errors that are sometimes as large as one order of magnitude, and size effects or altered boundary conditions of the samples. Direct measurements of K_s are generally difficult for undisturbed samples taken in the field. In addition, K_s is usually very sensitive to the saturated water content, since small errors in the water content near saturation can lead to large errors in K_s. Mallants et al. (1997) compared saturated hydraulic conductivities of three different undisturbed soils and reported average value of 334, 127, and 11.8 cm day^{-1} for small (5 cm long, 5 cm diameter), intermediate (20 cm long, 20 cm diameter), and large (100 cm long, 30 cm diameter) soil columns, respectively, taken from the same field. Because of the above difficulties, we decided to estimate K_s from the field–measured soil water content and infiltration data using the parameter estimation features of HYDRUS–2D.

Solute Transport

The physical non–equilibrium convection–dispersion model, also known as the mobile–immobile (MIM) or two–region model, for transport of non–reactive solute in variably saturated porous media is given by (van Genuchten and Wagenet, 1989; Clothier et al., 1998):

$$\frac{\partial(\theta_m C_m)}{\partial t} + \theta_{im}\frac{\partial C_{im}}{\partial t} = \frac{\partial}{\partial x_i}\left(\theta_m D_{ij}\frac{\partial C_m}{\partial x_j}\right) - \frac{\partial(q_i C_m)}{\partial x_i} \tag{6}$$

$$\theta_{im}\frac{\partial C_{im}}{\partial t} = \omega(C_m - C_{im}) \tag{7}$$

where

θ_m = mobile water content ($L^3 L^{-3}$)
θ_{im} = immobile water content ($L^3 L^{-3}$)
C_m = resident solute concentrations in the mobile region (ML^{-3})
C_{im} = resident solute concentrations in the immobile region (ML^{-3})
ω = first–order exchange coefficient (T^{-1})
q_i = volumetric flux (LT^{-1})
D_{ij} = dispersion coefficient tensor ($L^2 T^{-1}$) defined as follows:

$$\theta_m D_{ij} = D_T|q|\delta_{ij} + (D_L - D_T)\frac{q_i q_j}{|q|} + \theta_m D_o \tau_o \delta_{ij} \tag{8}$$

where

D_o = ionic or molecular diffusion coefficient in free water ($L^2 T^{-1}$)
τ_o = tortuosity factor (dimensionless)
δ_{ij} = Kronecker delta function (dimensionless)
D_L = longitudinal dispersivity (L)
D_T = transverse dispersivity (L).

Please note that equation 6 simplifies to the standard convection–dispersion equation (CDE) when no immobile water is present ($\theta_{im} = 0$).

Initial and Boundary Conditions

Measured bromide concentrations and soil water contents, the latter taken with a neutron probe, before the experiments were used as initial conditions within the flow domain. A constant pressure head (surface ponding, h_o in fig. 4) was specified as the upper boundary condition in the furrow during irrigation, while an atmospheric boundary condition was used after irrigation (during redistribution) as:

$$\left| K\left(K_{ij}^A \frac{\partial h}{\partial x_j} + K_{iz}^A\right) n_i \right| \le E \tag{9}$$

$$h_A \le h \le h_s \tag{10}$$

where

E = potential evaporation rate
n_i = components of the outward unit vector
h_A and h_s = minimum and maximum pressure heads, respectively, allowed under the prevailing soil conditions.

The value for h_A is determined from the equilibrium conditions between soil water and atmospheric water vapor, whereas h_s is usually set to zero. In this study, h_A was fixed at –15 bar, being the equilibrium value with a soil surface water content of 0.09 cm^3 cm^{-3} as measured at the end of the experiments. The average of the reference and estimated evapotranspiration rates was used as the atmospheric boundary condition.

A Cauchy condition was used for the upper boundary condition for solute transport, while free–drainage conditions for both water and solute were applied to the lower boundary of the domain (fig. 4). No–flux boundary conditions were applied to both sides of the flow domain. Measured furrow cross–sections as shown in figure 1, not the best fits, were used to define the upper section of the transport domain for each experimental plot. A finer grid (~0.5 cm) was used near the soil surface, and a much coarser grid (~4 cm) was specified at the bottom of the domain.

Inverse Optimization

The inverse problem was based on numerical solutions of the Richards equation (eq. 1) and the CDE or MIM convection–dispersion model (eqs. 6 and 7) using the Levenberg–Marquardt optimization procedure (Marquardt, 1963). In the inverse procedure, the unknown parameters are optimized by minimizing the objective function $\Phi(q,b)$ defined as (Simunek et al., 1999b):

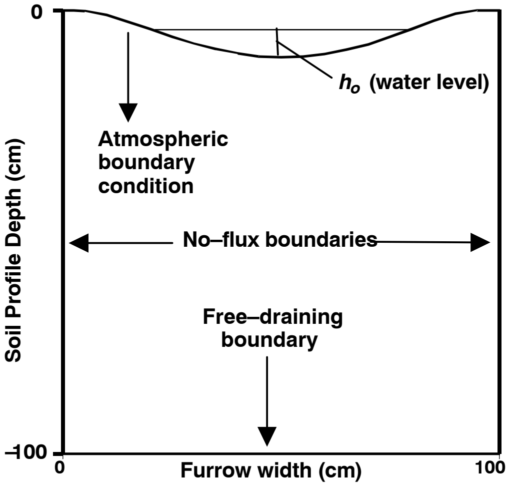

Figure 4. Applied water and solute boundary conditions for the specified soil profiles.

$$\Phi(q,b)=\sum_{j=1}^{m}v_j\sum_{i=1}^{n}w_{ij}[q_j^*(x,z,t_i)-q_j(x,z,t_i,b)]^2 \qquad (11)$$

where

n = number of observations for the jth measure–ment set (e.g., water contents, infiltrations, concentrations, ...)

$q_i^*(x,z,t_i)$ = specific measurements at time t_i, location x, and depth z

$q_i(x,z,t_i,b)$ = corresponding model predictions obtained with the vector of optimized parameters b = (D_L, D_T, ω, θ_{im}, ...)

v_j and w_{ij} = weights associated with a particular measurement set or point, respectively.

Weighting coefficients w_{ij} were assumed to be equal to 1, while the v_j values were determined according to Clausnitzer and Hopmans (1995).

Measured soil water contents, infiltration data, and bromide concentrations were used in the inverse optimization to estimate simultaneously K_s and two CDE (i.e., D_L and D_T) or four MIM transport parameters (i.e., D_L,D_T, ω, and θ_{im}). Other parameters (notably the VG soil hydraulic parameters) during the optimization were fixed at their values given in table 1. Each inverse simulation was run at least three times with different initial estimates to increase the probability of finding the global minimum of the objective function. Still, we understand that with the limited amount of measured data available, particularly bromide concentrations, and the many transport parameters to be estimated, no guarantee exists that a unique set of K_s and transport parameters was obtained. In this study, we used both the CDE and MIM approaches to see whether or not the two–region transport model would improve the predictions.

K_s and solute transport parameters were estimated simultaneously since this approach takes advantage of crossover effects between the water flow and solute transport state variables and parameters (Sun and Yeh, 1990). This method uses simultaneously all available information and hence should yield smaller estimation errors than sequential estimation (Mishra and Parker, 1989; Simunek et al., 2002). The current version of HYDRUS–2D is capable of simultaneously estimating up to 15 different soil hydraulic, root water uptake, and/or transport parameters. However, we recommended to rarely, if ever, optimize such a large number of parameters. The number of parameters that can be simultaneously optimized depends on the availability of measured data used in the objective function and on the uncertainty in the estimated parameters.

Results and Discussion

Final optimized values of the saturated hydraulic conductivity and CDE and MIM transport parameters for the different experiments are summarized in table 2. Notice that the optimized parameters and sum of squared residuals (SSQ) for the CDE and MIM transport models are very similar for the different plots (except for D_L in plot 1).

The estimated values for K_s were more or less the same for all experiments, except for plot 5, whose K_s was about two times larger than for the other experiments. These results are consistent with field observations indicating that during the second irrigation the same amounts of water infiltrated in almost the same time in plots 3 and 5, which had water levels of 14 and 10 cm, respectively, whereas a shorter application time was observed for plot 5 notwithstanding its lower water level of 10 cm. The estimated K_s values are close to those reported by Carsel and Parrish (1988) and Schaap et al. (1998) for sandy loam soils. The optimization results indicated very little correlation between K_s and the other parameters. Correlation coefficients were generally less than about 0.05 for the different plots.

Contrary to recent studies (e.g., Jacques, 2000; Ventrella et al., 2000), which suggest that the presence of immobile water is important for modeling field–scale solute transport, our analysis produced relatively low values for immobile water content (θ_{im}) (table 2), thus indicating that immobile

Table 2. Summary of the optimized saturated hydraulic conductivity (K_s) and CDE and MIM transport parameters for the different experiments. Optimized values for the CDE runs are given in parentheses.

	Experiment	K_s (cm min^{-1})	θ_{im} (cm^3 cm^{-3})	ω (min^{-1})	D_L (cm)	D_T (cm)	SSQ (–)	R^2 (–)
SD[a]	Plot 1 (6 cm)	0.0394 (0.0389)	0.029	19.52	32.8 (18.3)	0.07 (0.03)	1.69 (1.69)	0.99 (0.99)
	Plot 2 (10 cm)	0.0396 (0.0392)	0.010	0.10	16.8 (17.0)	0.81 (0.40)	3.48 (4.22)	0.99 (0.99)
	Plot 3 (14 cm)	0.0497 (0.0497)	0.057	4.11	13.5 (12.5)	0.05 (0.04)	6.40 (6.32)	0.98 (0.98)
SWS[b]	Plot 4 (6 cm)	0.0456 (0.0436)	0.010	7.87	7.9 (8.3)	0.04 (0.07)	8.73 (8.93)	0.99 (0.99)
	Plot 5 (10 cm)	0.0957 (0.0996)	0.020	11.20	3.7 (2.6)	2.10 (2.20)	3.23 (3.50)	0.99 (0.99)
CV (%)		43.9 (47.5)	76.8	86.4	74.7 (55.1)	145 (170)	—	—

[a] Same duration (SD) experiments.
[b] Same amount of applied water and solute (SWS) experiments.

water did not play a major role in our study, and hence that advection and dispersion were the main transport processes. This may be due in part to the coarse texture (sandy loam) of the soil studied. Values for θ_{im} for the various plots varied between 0.010 and 0.057 cm^3 cm^{-3}. Unlike θ_{im}, the first–order exchange coefficient (ω) values (table 2) were found to vary highly between the different experiments (CV = 86.4%), with the estimated values being about one to two orders of magnitude higher than those reported in the literature for both laboratory (e.g., Jacobsen et al., 1992; Mallants et al., 1996) and field studies (Jaynes et al., 1995; Jacques et al., 2002). The high values reflect rapid solute exchange between the mobile and immobile regions. This suggests that even if some immobile water is present, solute exchange between the two regions would be so rapid that the transport process would become macroscopically indistinguishable from a CDE–type process in which advection and dispersion dominate.

The highly transient nature of the 2–D infiltration processes may well have contributed to the relatively standard convective–dispersive nature of the transport processes in our study. Other studies in which mobile–immobile transport processes were investigated and/or MIM parameters were derived usually involved 1–D studies, mostly during flow conditions at or close to steady–state (Nkedi–Kizza et al., 1983; Seyfried and Rao, 1987; Jaynes et al., 1995; Mallants et al., 1996; among others). Additional 2–D water flow and transport studies under transient infiltration conditions may be needed to confirm our results; we are unaware of any other studies of this type in the literature. We note that our optimizations never converged when we used very low initial guesses for ω (less than 0.001 min^{-1} for some experiments, and less than 0.1 min^{-1} for others). Also, spatial variability in the soil hydraulic properties made it difficult to draw conclusions about the effects of the water level on θ_{im} and ω. Additional measurements, particularly of solute concentrations at more frequent time levels, perhaps could have produced more precise optimized parameters.

The optimized D_L values ranged from 2.6 to 32.8 cm, while D_T values varied between 0.03 and 2.20 cm (table 2). D_L values were somewhat larger than those typically obtained from 1–D laboratory transport experiments during steady–state flow. However, they were fairly similar to values previously reported by Bowman and Rice (1986) and Jaynes et al. (1988) for field experiments at the same field site involving intermittent and continuous flood irrigation regimes, respectively. For instance, D_L values (as estimated with the one–dimensional CDE) obtained by Jaynes et al. (1988) varied between 13.8 to 22.8 cm. Estimated D_L and D_T values were comparable with those reported earlier by Forrer et al. (1999) for a 2–D field–scale study under steady–state flow conditions. The relatively large optimized values for D_L and D_T observed for several plots were likely due to inherent 2–D behavior of the solute transport process and more lateral flow spreading in the furrows. They also reflect the natural heterogeneity of our field site, spatial variability in soil water contents, and perhaps our somewhat lower water contents as compared to the experimental conditions of Forrer et al. (1999). The relatively low D_T values for some of our plots could also have been compensated somewhat by the large D_L values (correlation coefficients between D_L and D_T were found to be about 0.25). Overall, however, the relatively large confidence intervals for the optimized D_T values indicate that our experiments did not provide enough information to reliably estimate this parameter.

Overall, the obtained D_L values for the drier plots (SD experiments) were higher than those for the SWS plots with the higher soil water contents. This is consistent with theoretical analyses by Russo (1993, 1998), who showed that the dispersivity should increase with decreasing soil water contents and increasing spatial variability in the soil water content. D_L also showed some dependency on the water level in the furrow and the water/solute application time. Higher values for D_L were obtained for the SD experiments. It is difficult to discern if this difference is caused by differences in the water level and/or application time, or due to variability in the soil properties.

The relatively large estimated D_T value for plot 5 may have been caused by increased lateral flow in this plot. As demonstrated by Abbasi et al. (2003), observed concentrations, particularly in the SWS plots, showed considerable lateral solute spreading. In addition, D_T values showed larger CVs as compared to the other optimized parameters (table 2). Previous sensitivity analyses indicate that numerical models are more sensitive to changes in D_T (Forrer et al., 1999) than in D_L (Forrer et al., 1999; Ventrella et al, 2000). Furthermore, both theoretical and experimental investigations have shown that field–scale dispersivities are several orders of magnitudes larger than laboratory–scale values for the same porous medium (Gelhar et al., 1992) and increase with the scale of observation (Fried, 1975; Gelhar et al., 1992). Observed longitudinal dispersivities for 59 different soils and aquifers ranged from 10^{-2} to 10^4 m for scales ranging from 10^{-1} to 10^5 m (Gelhar et al., 1992).

Measured cumulative infiltration rates, soil water contents, and solute concentrations from all five experimental plots are compared in figure 5 with predicted values as calculated with the optimized parameters. Measured infiltration data matched the predicted values reasonably well (R^2 was about 0.95), with agreement between measured and predicted water contents and concentrations being somewhat less. Water contents were mostly overestimated, and concentrations were underestimated. Overestimation of water contents could be due to possible overestimation of the laboratory–measured θ_s values). Including θ_s and other soil hydraulic parameters in the optimization could well have improved the model predictions. However, as indicated earlier, we felt it is important to limit as much as possible the number of unknown parameters in view of the limited amount of measured data and the relatively high sensitivity of the parameter estimation technique to the number of unknowns (Simunek et al., 1999b). Only K_s was included in the optimization procedure since we did not have direct field measurements of this parameter. The MIM and CDE transport models showed more or less the same agreement between observed and predicted values (fig. 5). Note that the R^2 values in figure 5 represent regressions of measured versus predicted results for all of the data pertaining to the five optimized plots, whereas the R^2 values in table 2 hold for specific data types (infiltration, soil water content, and concentration) used in the individual optimizations.

Selected comparisons between measured and model–predicted soil water contents and solute concentrations are presented in figures 6 and 7, respectively. Plot 1 was selected for these comparisons because of relatively large differences between the optimized CDE and MIM transport parameters

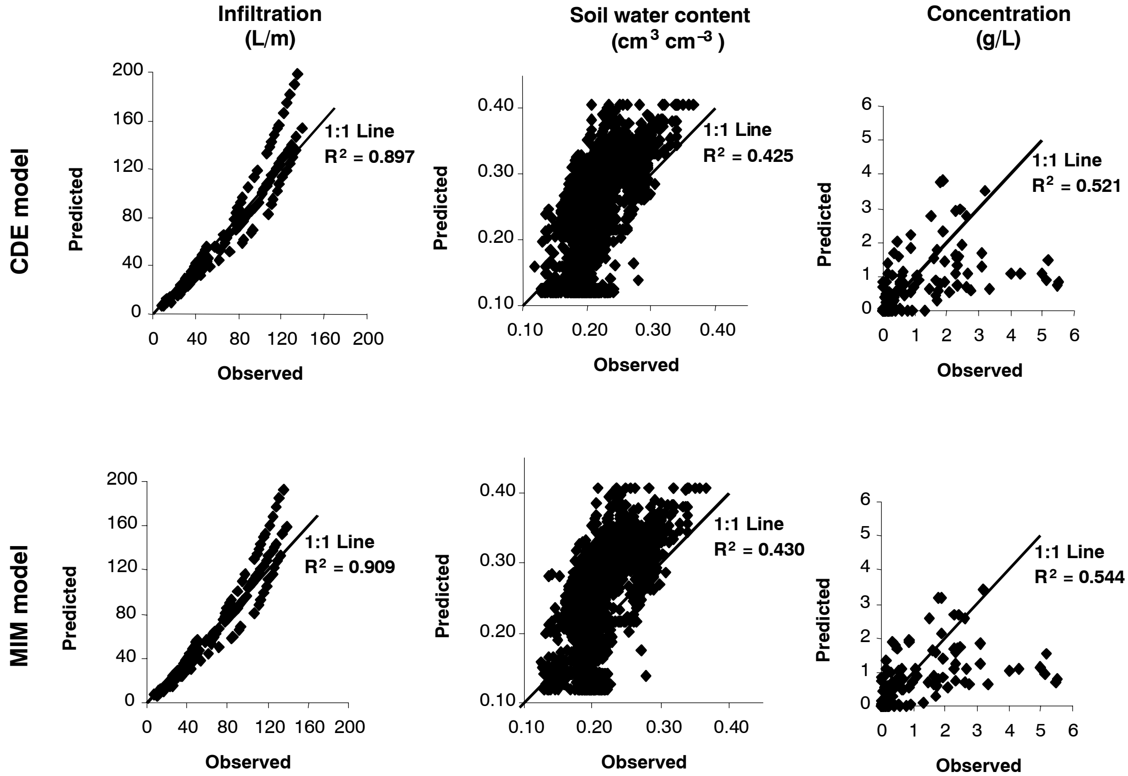

Figure 5. Measured versus predicted (using the CDE and MIM transport models) cumulative infiltration rates, soil water contents, and solute concentrations for all experimental plots.

for this plot (table 2). Relatively good agreement was found between observed and calibrated soil water contents in the redistribution phase (figs. 6b and 6c), whereas water contents were overestimated during infiltration (fig. 6a) and also in the drier conditions (fig. 6d). Results for the second irrigation event (not shown) were more or less the same as those for the first irrigation shown in figure 6.

Agreement between measured and predicted solute concentration distributions was somewhat poor near the soil surface, where the model underestimated concentrations, but it was much better in deeper layers (fig. 7). In spite of underestimating peak concentrations, the model estimated the observed solute concentration fronts at different times very well. We believe that one–dimensional soil water content and solute concentration breakthrough curves could have provided a better and more cogent comparison between model predictions and field measurements. Also, notwith–standing the large discrepancy between the optimized MIM

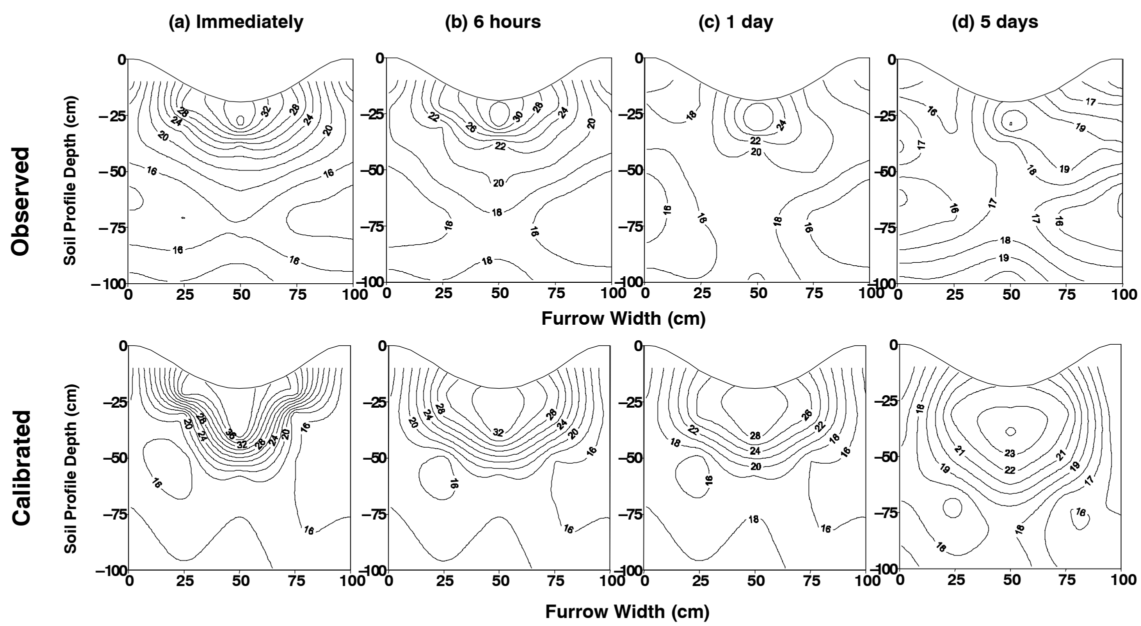

Figure 6. Measured and calibrated soil water contents in plot 1 at different times after the first irrigation event.

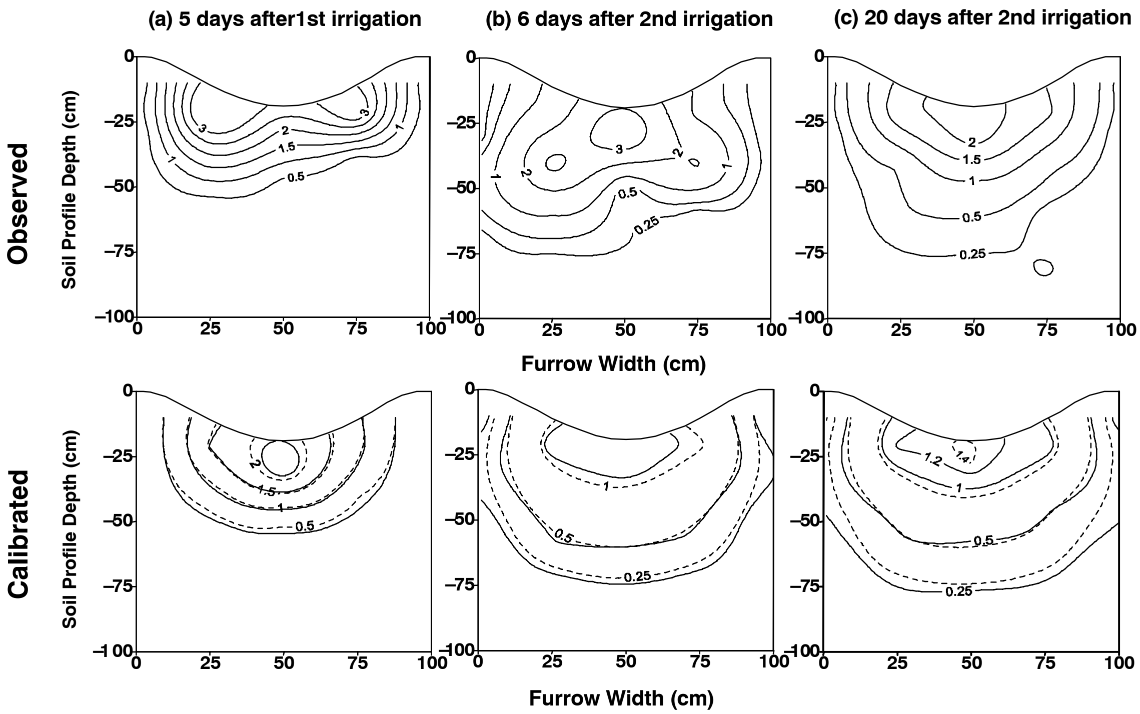

Figure 7. Measured and calibrated solute concentrations in plot 1 at different soil sampling times (dashed lines = CDE, and continuous lines = MIM).

and CDE dispersivity values for plot 1 (table 2), no obvious differences were found between predictions with the CDE and MIM transport models (fig. 7). This again indicates relatively low sensitivity of solute transport models to the longitudinal dispersivity, as was previously shown also by Ventrella et al. (2000) and Forrer et al. (1999) for one– and two–dimensional field–scale studies, respectively.

Conclusions

The HYDRUS–2D code in combination with the Levenberg–Marquardt optimization algorithm was used to inversely estimate the saturated hydraulic conductivity and CDE and MIM transport parameters from several field–scale water flow and solute transport experiments carried out under transient conditions. The optimized parameters, particularly the saturated hydraulic conductivity and the longitudinal and transverse dispersivities, corresponded well with values reported in the literature for field–scale studies. Results indicate that immobile water did not play an important role, perhaps because of the relatively coarse texture of our field site. Immobile water contents were more or less the same for the different experiments, giving an average value of only 0.025 $cm^3 \, cm^{-3}$. The first–order mass transfer coefficient was higher than those reported for most 1–D analyses on soil columns (Seyfried and Rao, 1987; Mallants et al., 1996) and field studies (Jaynes et al., 1995; Jacques, 2000). This reflects rapid exchange of solute with any immobile water that is present, and hence indicates that the effects of immobile water were relatively minimal in our study. These results are consistent with the fact that only minor differences were found between the CDE and MIM solute concentration predictions.

Estimated values for the longitudinal dispersivity were larger than those reported earlier for laboratory soil columns, but similar to those measured for field studies (Bowman and Rice, 1986; Jaynes et al., 1988; Forrer et al., 1999). We believe that our somewhat higher values are related to having slightly lower water contents and more irregular flow patterns than previous studies and also uncertainty in estimating several parameters, simultaneously. Longitudinal dispersivities showed some dependency on the water level in the furrows and the water/solute application time, but no clear effects were found of the water level on the transverse dispersivity, the immobile water content, and the mass transfer coefficient. Agreement between model predictions and measured infiltration data was generally satisfactory, while it was relatively poor for soil water contents and solute concentrations. Soil water contents were somewhat overestimated during the infiltration and later stages of redistribution when the soil dried out, while solute concentrations were underestimated near the soil surface.

Simultaneous estimation of soil hydraulic and transport parameters has the advantage that this can be done in a single step. The method, however, may sometimes lead to inaccurate transport parameters since the objective function is defined in terms of both hydraulic and transport data. Large hydraulic residuals could then compensate (or overshadow) small transport residuals, and vice versa. The final outcome of the optimization process then depends very much on what weights are given to the particular data sets.

The present simulations were carried out assuming a homogeneous soil profile. Accounting for soil layering and implementing a scaling method to describe spatial variability in the soil hydraulic and transport properties and consequently estimating the invoked parameters with the classical sequential estimation of hydraulic parameters followed by solute transport parameters will further improve the predictions. One concern we had during analysis of our data was the required computational time for the 2–D water flow and solute transport calculations, especially during inverse analyses of the heterogeneous case. Depending on the initial estimates of the unknown parameters, optimization required up to several days on a Pentium III PC. In addition, accurate evaluation of soil hydraulic and solute transport properties from field–scale data, which are subject to considerable spatial and temporal variability, requires extensive data collection. For these reasons, it is important to measure as many parameters as possible independently, especially when limited or highly variable field data are available.

Acknowledgements

The authors are grateful to Jack Jobes of the George E. Brown Jr. Salinity Laboratory, Riverside, California, for his help in analyzing soil samples for soil water retention curves and saturated hydraulic conductivity. This study was partially supported by SAHRA (Sustainability of Semi–Arid Hydrology and Riparian Areas) under the STC Program of the National Science Foundation, Agreement No. EAR–9876800.

References

Abbasi, F., F. J. Adamsen, D. J. Hunsaker, J. Feyen, P. Shouse, and M. Th. van Genuchten. 2003. Effects of flow depth on water flow and solute transport in furrow irrigation: Field data analysis. *J. Irrig. and Drainage Eng.* 129(4): 237–246.

Addiscott, T. M., and R. J. Wagenet. 1985. Concepts of solute leaching in soils: A review of modeling approaches. *European J. Soil Science* 36(3): 411–424.

Allen, R. G., M. Smith, A. Perrier, and L. S. Pereira. 1994. An update for the definition of reference evapotranspiration. *ICID Bulletin* 43(2): 1–34.

Biggar, J. W., and D. R. Nielsen. 1976. Spatial variability of the leaching characteristics of a field soil. *Water Resources Research* 12(1): 78–84.

Bowman, R. S., and R. C. Rice. 1986. Transport of conservative tracers in the field under intermittent flood irrigation. *Water Resources Research* 22(11): 1531–1536.

Bresler, E., G. Dagan, R. J. Wagenet, and A. Laufer. 1984. Statistical analysis of salinity and texture effects on spatial variability of soil hydraulic conductivity. *SSSA J.* 48(1): 16–25.

Carsel, R. F., and R. S. Parrish. 1988. Developing joint probability distributions of soil water retention characteristics. *Water Resources Research* 24(5): 755–769.

Clausnitzer, V., and J. W. Hopmans. 1995. Non–linear parameter estimation: LM–OPT. General–purpose optimization code based on the Levenberg–Marquardt algorithm. Land, Air, and Water Resources Paper No. 100032. Davis, Cal.: University of California.

Clothier, B. E., I. Vogeler, S. R. Green, and D. R. Scotter. 1998. Transport in unsaturated soil: Aggregates, macropores, and exchange. In *Physical Nonequilibrium in Soils: Modeling and Application*, 273–295. H. M. Selim and L. Ma, eds. Chelsea, Mich.: Ann Arbor Press.

Forrer, I., R. Kasteel, M. Flury, and H. Fluhler. 1999. Longitudinal and lateral dispersion in an unsaturated field soil. *Water Resources Research* 35(10): 3049–3060.

Forsyth, P. A., Y. S. Wu, and K. Pruess. 1995. Robust numerical methods for saturated–unsaturated flow with dry initial conditions. *Advances in Water Resources* 18(1): 25–38.

Fried, J. J. 1975. *Groundwater Pollution*. New York, N.Y.: Elsevier.

Gelhar, L. W., C. Welty, and K. R. Rehfeldt. 1992. A critical review of data on field–scale dispersion in aquifers. *Water Resources Research* 28(7): 1955–1974.

Gribb, M. M. 1996. Parameter estimation for determining hydraulic properties of a fine sand from transient flow measurements. *Water Resources Research* 32(7): 1965–1974.

Jacobsen, O. H., F. J. Leij, and M. Th. van Genuchten. 1992. Parameter determination for chloride and tritium transport in undisturbed lysimeters during steady flow. *Nordic Hydrology* 23(2): 89–104.

Jacques, D. 2000. Analysis of water flow and solute transport at the field scale. PhD diss. No. 454. Leuven, Belgium: Katholieke Universiteit Leuven, Fac. Landbouwkundige en Toegepaste Biologische Wetenschappen.

Jacques, D., J. Simunek, A. Timmerman, and J. Feyen. 2002. Calibration of Richards' and convection–dispersion equations to field–scale water flow and solute transport under rainfall conditions. *J. Hydrology* 259: 15–31.

Jarvis, N. J., P. E. Jonsson, P. E. Dik, and I. Messing. 1991. Modeling water and solute transport in macroporous soil: I. Model description and sensitivity analysis. *European J. Soil Science* 42(1): 59–70.

Jaynes, D. B., R. S. Bowman, and R. C. Rice. 1988. Transport of a conservative tracer in the field under continuous flood irrigation. *SSSA J.* 52(3): 618–624.

Jaynes, D. B., S. D. Logsdon, and R. Horton. 1995. Field method for measuring mobile/immobile water content and solute transfer rate coefficient. *SSSA J.* 59(2): 352–356.

Kees, C. E., and C. T. Miller. 2001. Higher order integration methods for two–phase flow. *Advances in Water Resources* 25(2): 159–177.

Kodesova, R., M. M. Gribb, and J. Simunek. 1998. Estimating soil hydraulic properties from transient cone permeameter data. *Soil Science* 163(6): 436–453.

Kodesova, R., S. E. Ordway, M. M. Gribb, and J. Simunek. 1999. Estimating of soil hydraulic properties with cone permeameter: Field studies. *Soil Science* 164(8): 527–541.

Loretta, Y., and G. Wu. 1999. Numerical simulation of four heavy metals in kaolinite clay. *J. Environ. Eng.* 125(4): 314–324.

Mallants, D., M. Vanclooster, and J. Feyen. 1996. Transect study on solute transport in a macroporous soil. *Hydrological Processes* 10(1): 55–70.

Mallants, D., B. P. Mohanty, A. Vervoort, and J. Feyen. 1997. Spatial analysis of saturated hydraulic conductivity in a soil with macropores. *Soil Technology* 10(2): 115–131.

Marquardt, D. W. 1963. An algorithm for least squares estimation of non–linear parameters. *J. Ind. Appl. Math.* 11: 431–441.

Mishra, S., and J. C. Parker. 1989. Parameter estimation for coupled unsaturated flow and transport. *Water Resources Research* 25(3): 385–396.

Mohanty, B. P., R. S. Bowman, M. H. Hendrickx, and M. Th. van Genuchten. 1997. New piecewise–continuous hydraulic functions for modeling preferential flow in an intermittent–flood–irrigated field. *Water Resources Research* 33(9): 2049–2063.

Mohanty, B. P., R. S. Bowman, M. H. Hendrickx, J.Simunek, and M. Th. van Genuchten. 1998. Preferential transport of nitrate to a tile drain in an intermittent–flood–irrigated field: Model development and experimental evaluation. *Water Resources Research* 34(5): 1061–1067.

Mualem, Y. 1976. A new model for predicting the hydraulic conductivity of unsaturated porous media. *Water Resources Research* 12(3): 513–522.

Neuman, S. P., R. A. Feddes, and E. Bresler. 1975. Finite element analysis of two–dimensional flow in soils considering water uptake by roots: I. Theory. *SSSA Proc.* 39(2): 224–230.

Nkedi–Kizza, P., J. W. Biggar, M. Th. van Genuchten, P. J. Wierenga, H. M. Selim, J. M. Davidson, and D. R. Nielsen. 1983. Modeling tritium and chloride36 transport through an aggregated oxisol. *Water Resources Research* 19(3): 691–700.

Richards, L. A. 1931. Capillary conduction of liquids through porous medium. *Physics* 1: 318–333.

Russo, D. 1993. Stochastic modeling of macrodispersion for solute transport in a heterogeneous unsaturated porous formation. *Water Resources Research* 29(2): 383–397.

Russo, D. 1998. Stochastic analysis of flow and transport in unsaturated heterogeneous porous formations: Effects of variability in water saturation. *Water Resources Research* 34(4): 569–581.

Russo, D., J. Zaidel, and A. Laufer. 1998. Numerical analysis of flow and transport in a three–dimensional partially saturated heterogeneous soil. *Water Resources Research* 34(6): 1451–1468.

Schaap, M. G., F. J. Leij, and M. Th. van Genuchten. 1998. Neural network analysis for hierarchical prediction of soil hydraulic properties. *SSSA J*. 62(4): 847–855.

Schaap, M. G., F. J. Leij, and M. Th. van Genuchten. 2001. ROSETTA: A computer program for estimating soil hydraulic parameters with hierarchical pedotransfer functions. *J. Hydrology* 251: 163–176.

Segol, G. 1994. *Classic Groundwater Simulations: Proving and Improving Numerical Models*. Englewood Cliffs, N.J.: Prentice–Hall.

Seyfried, M. S., and P. S. C. Rao. 1987. Solute transport in undisturbed columns of an aggregated tropical soil: Preferential flow effects. *SSSA J*. 51(6): 1434–1444.

Shao, M., R. Horton, and R. K. Miller. 1998. An approximate solution to the convection–dispersion equation of solute transport in soil. *Soil Science* 163(5): 339–345.

Simunek J., and M. Th. van Genuchten. 1994. The CHAIN–2D code for simulating the two–dimensional movement of water, heat, and multiple solutes in variably saturated porous media. Research Report 136. Riverside, Cal.: USDA–ARS, George E. Brown Jr. Salinity Laboratory.

Simunek, J., and M. Th. van Genuchten. 1996. Estimating unsaturated soil hydraulic properties from tension disc infiltrometer data by numerical inversion. *Water Resources Research* 32(9): 2683–2696.

Simunek, J., and M. Th. van Genuchten. 1997. Estimating unsaturated soil hydraulic properties from multiple tension disc infiltrometer data. *Soil Science* 162(6): 383–398.

Simunek, J., M. Sejna, and M. Th. van Genuchten. 1998. The HYDRUS–1D software package for simulating the one–dimensional movement of water, heat, and multiple solutes in variably saturated media, Version 2.0. IGWMC–TPS–70. Golden Colo.: Colorado School of Mines, International Ground Water Modeling Center.

Simunek, J., M. Sejna, and M. Th. van Genuchten. 1999a. The HYDRUS–2D software package for simulating the two–dimensional movement of water, heat, and multiple solutes in variably saturated media, Version 2.0, IGWMC–TPS–70. Golden Colo.: Colorado School of Mines, International Ground Water Modeling Center.

Simunek, J., R. Kodesova, M. M. Gribb, and M. Th. van Genuchten. 1999b. Estimating hysteresis in the soil water retention function from cone permeameter experiments. *Water Resources Research* 35(5): 1329–1345.

Simunek, J., D. Jacques, J. W. Hopmans, M. Inoue, M. Flury, and M. Th. van Genuchten. 2002. Solute transport during variably–saturated flow – Inverse methods. Chapter 6.6 in *Methods of Soil Analysis: Part 1. Physical Methods*, 1435–1449. 3rd ed. J. H. Dane and G. C. Topp, eds. Madison, Wisc.: SSSA.

Sulekha, D. K., and W. H. M. Duijnisveld. 1998. Two–phase reactive solute transport simulation in unsaturated zone. *J. Irrig. Drainage Eng*. 124(3): 140–147.

Sun, N. Z., and W. W. G. Yeh. 1990. Coupled inverse problems in groundwater modeling: 1. Sensitivity analysis and parameter identification. *Water Resources Research* 26(10): 2507–2525.

van Genuchten, M. Th. 1980. A closed–form equation for predicting the hydraulic conductivity of unsaturated soils. *SSSA J*. 44(5): 892–898.

van Genuchten, M. Th., and E. A. Sudicky. 1999. Recent advances in vadose zone flow and transport modeling. In *Vadose Zone Hydrology: Cutting Across Disciplines*, 155–193. M. B. Parlange and J. W. Hopmans, eds. New York, N.Y.: Oxford University Press.

van Genuchten, M. Th., and R. J. Wagenet. 1989. Two?site/two?region models for pesticide transport and degradation: Theoretical development and analytical solutions. *SSSA J*. 53(5): 1303?1310.

van Genuchten, M. Th., F. J. Leij, and S. R. Yates. 1991. The RETC code for quantifying the hydraulic functions of unsaturated soils. Report No. EPA/600/2–91/065. Ada, Okla.: U.S. Environmental Protection Agency, R. S. Kerr Environmental Research Laboratory.

Ventrella, D., B. P. Mohanty, J. Simunek, N. Losavio, and M. Th. van Genuchten. 2000. Water and chloride transport in a fine–textured soil: Field experiments and modeling. *Soil Science* 165(8): 624–631.

Wang, D., S. R. Yates, J. Simunek, and M. Th. van Genuchten. 1997. Solute transport in simulated conductivity fields under different irrigations. *J. Irrig. Drainage Eng*. 123(5): 336–343.

Wu, G., and S. T. Chieng. 1995a. Modeling multicomponent reaction chemical transport in non–isothermal unsaturated/saturated soils: Part 1. Mathematical model development. *Trans. ASAE* 38(3): 817–826.

Wu, G., and S. T. Chieng. 1995b. Modeling multicomponent reaction chemical transport in non–isothermal unsaturated/saturated soils: Part 2. Numerical simulation. *Trans. ASAE* 38(3): 827–838.